Computer Modeling in Engineering & Sciences

Tech Science Press

DOI: 10.32604/cmes.2022.018507

ARTICLE

A Discrete Numerical Study of the Effect of the Thickness and the Porosity of the Sand Cushion on the Impact Response Due to the Rockfall

Song Yuan[1], Peng Zhao[2,*], Liangpu Li[1,*], Xibao Wang[1], Jun Liu[3] and Bo Zhang[4]

[1]Sichuan Communication Surveying & Design Institute Co., Ltd., Chengdu, 610065, China

[2]Key Laboratory of Deep Underground Science and Engineering (Ministry of Education), College of Architecture and Environment, Sichuan University, Chengdu, 610065, China

[3]Institute of New Energy and Low-Carbon Technology, Sichuan University, Chengdu, 610065, China

[4]Institute of Science and Technology, China Three Gorges Corporation, Beijing, 100038, China

[*]Corresponding Authors: Peng Zhao. Email: scu_zhaopeng@163.com; Liangpu Li. Email: llp_scu@163.com

Received: 29 July 2021 Accepted: 23 September 2021

ABSTRACT

The prevention and the reduction of the rockfall are the common measures of the prevention and the reduction of disasters. When the rock-shed resists the impact of the rockfall, the force that acts on the structure consists of the cushion dead load and the impact-induced load, of which the dynamic process of the propagation of the impact-induced load is complex. Therefore, we conducted a numerical study to investigate the impact of the rockfall. Considering the highly discrete characteristic of the sand, we developed a numerical model on the basis of the discrete element method (DEM). The numerical model, which simulation results were validated by the results of real-scale experiments, was used to investigate the dynamic response of the impact force of the rockfall and the transmission of the impact force under the different magnitude of the falling height and the different thickness of the sand cushion. The results of our study indicated that the cushion thickness had little effect on the impact of the rockfall, and the dense sand cushion generated higher impact force than did the loose sand cushion. Although the high thickness enhanced the buffer performance of the sand cushion, the additional force induced by the dead load of sand cushion was significant. Therefore, to determine the appropriate thickness of the sand cushion, we suggested designers consider the buffer performance and the dead load of the sand cushion. The analysis presented in this paper provided a practical estimation of the impact-induced force of the thick sand cushion.

KEYWORDS

Rockfall; impact; DEM; sand cushion; thickness; porosity; impact force; bottom force

1 Introduction

The topographical and the geological characteristics of western China are extremely complex. In the region, the earthquake, the extreme weather, and secondary disasters occur frequently. The rockfall is a common geological hazard, which occurs unexpectedly [1]. Regardless of the scale of

the rockfall, the urgent attention is required to avoid casualties and the economic loss. Rock-sheds have been widely applied as protective structures [2]. According to the survey that was conducted by the Sichuan Communication Surveying & Design Institute on the rock-sheds and the open-cut tunnels that were built after the Wenchuan Earthquake, nearly 80% of the structural damage to the rock-sheds or the tunnels was induced by the rockfall [3,4]. Therefore, the ability of rock-shed to resist the impact of the rockfall needs to be deeply explored.

To improve the structural design, researchers have conducted a series of large-scale experiments, and discussed the effect of the structural type [5–7] and construction materials [2,8] on the impact resistance of structures. In addition to the structural design, the cushion filled on the slab also plays an important role on the impact resistance of structures. The properties of the cushion, such as the porosity, the thickness, the density, and the grain size, were investigated by laboratory or prototype experiments [2,4,9–12]. On the basis of the experiments, researchers obtained some sound achievements, which may be used to guide the rock-shed design.

The purpose of the cushion is to reduce the impact force of the rockfall and to protect the structure. During the impact, the impact force is transmitted through the cushion before acting on the structure. The transmitted force is directly related to the structural design. Hence, on the basis of experimental results, researchers discussed the transmitted force. For example, by real-scale impact experiments, Calvetti et al. [9,13] suggested that the stress distribution on the plate should be computed by considering the dynamic amplification effect. Lambert et al. [10] designed small-scale experiments and investigated the effect of the grain gradation and the boundary condition on the transmitted force. On the basis of a series of laboratory tests, Kawahara et al. [11] found that the earth pressure at the bottom of the soil increased with the soil density and decreased with the thickness of the soil. The propagation of the impact-induced force through the cushion is a highly complex dynamic process. Unlike continuous materials, the sand is a typical granular material. Because the impact-induced force is mainly transmitted through the contact between particles, the properties of the sand cushion, such as the porosity and the stiffness, are determined by the grain shape, the size, and the density of the sand. Hence, it is difficult to clearly define the propagation of the impact-induced force through the sand cushion. Although researchers have conducted laboratory and large-scale experiments to study the impact force of the rockfall, the researchers considered the limited working condition and limited influencing factors. Some conclusions that were obtained by the researches remain unaddressed. At present, there are several calculation methods to estimate the impact force of the rockfall, such as the algorithm of the Japan Road Association, the recommendations by the ASTRA of Switzerland, and the Specifications for Design of Highway Subgrades of China [14]. Unfortunately, the calculation methods are unable to estimate the transmitted force, which is the primary concern of designers.

In recent years, supported by the development of the numerical analysis, the numerical simulation is a good technical tool to study the impact force of the rockfall. On the basis of a reliable model, several factors may be considered in the numerical simulation study, and some results have been achieved. Ouyang et al. [15] simulated the transient dynamic procedure of the impact of the rockfall and discussed the effects of various lightweight damping materials on the reduction of the impact force. Bhatti [16] developed a numerical model to study the energy dissipating capacity of the different thickness and density of expanded polystyrene cushions. Yan et al. [17] presented a numerical approach to reveal the influence of the rock shape on the impact force. More aforementioned numerical methods incorporated the finite element method (FEM). Although the maximum impact force can be approximated by the FEM, it is difficult to simulate the second wave [18]. The FEM treats the sand as a continuous material. At present, there is

no suitable constitutive model to describe the sand deformation behavior under the impact load. The sand cushion is composed of discrete particles. The discrete element method (DEM) is more appropriate than the FEM to simulate the sand cushion. Recently, researchers used the DEM to discuss the impact of the rockfall and the transmitted force [19]. Calvetti et al. [13] established a linear correlation between the impact force and the stress on the plate and described the dynamic amplification effect. Shen et al. [20] found that the shape of the rock block had little influence on the peak stress distribution on the bottom floor. The researches attempted to use the DEM to discuss the transmitted force; however, the researchers rarely consider the characteristics of the cushion in the model. Moreover, the estimation of the transmitted force is scarce.

To understand the impact response of the rockfall, especially the transmitted force, we conducted systematic numerical analysis. Firstly, we developed a three-dimensional DEM model in Particle Flow Code (PFC). Secondly, we validated the results of the numerical simulation by the results of real-scale experiments. On the basis of a reliable numerical model, we discussed the impact force and the transmitted force of the rockfall. The effects of the falling height, the thickness of the sand cushion, and the sand porosity were investigated. Finally, we explored the relationship between the cushion dead load and the impact-induced load of the thick sand cushion.

2 The DEM Method and the Validation of the Model

2.1 The DEM Method

The DEM for the simulation of granular materials was proposed by Cundall et al. [21]. The translational and rotational motions of each granular particle are described by the Newton's second law of motion as:

$$m\ddot{x} = F + mg, \tag{1}$$

$$M_i = I\dot{w}_i, \tag{2}$$

where m is the particle mass; x is the position of the particle centroid; F is the resultant force acting on the particle; g is the gravity acceleration vector; M_i is the resultant moment acting on the particle; ω_i is the angular velocity and I is the moment of inertia.

The interactions between particles can be calculated by the force-displacement law:

$$F_n = k_n u_n, \tag{3}$$

$$\Delta F_t = -k_t \Delta u_t, \tag{4}$$

where F_n and F_t is the normal and tangential contact force; k_n and k_t is the normal and tangential contact stiffness; u_n is the overlapping distance between the two particles; ΔF_t is computed incrementally from the relative tangential displacement Δu_t.

Compared to the deformation of a granular assembly, the particle deformation is very small. It is not necessary to calculate the particle deformation precisely to obtain a good approximation of the mechanical behaviour. Therefore, in PFC software, the particles are allowed to overlap one another at contact points. This overlapping behaviour takes the place of the particle deformation. The interactions between the particles are considered explicitly and the contact forces are defined as a function of the overlap. It should be noted, however, that these overlaps are small in relation to the particle sizes [21,22].

In the PFC software, the explicit finite difference method is used for the cyclic iterative solution. During every calculation cycle, the Newton's second law of motion is applied to every

particle and the force-displacement law is applied to every contact. Moreover, the positions of the particles and walls are updated constantly.

When developing a DEM model, the choice of the contact model is a key step. In this study, the linear model was employed to simulate the sand cushion, the contact between the sand cushion and the rockfall, and the contact between the sand cushion and the slab. In the PFC, the linear model consists of two parallel components, namely the linear component and the dashpot component. The linear component provides the linear elastic (no-tension) frictional behavior, and the dashpot component provides the viscous behavior (Fig. 1). Both components act on a vanishingly small area, thus, only transmit a force [22]. Further information on the linear model is available in the help document of the PFC3D software.

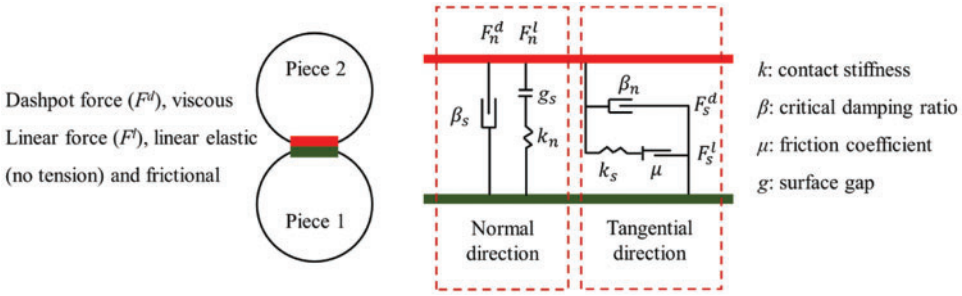

Figure 1: The behavioral and the rheological components of the linear model

Compared with continuum methods such as the FEM, the DEM simulates the actual mechanical properties of granular materials. There were three objects involved in the development of the DEM model to simulate the impact of the rockfall, namely, the rock block, the protective structure, and the sand cushion. The rock block was regarded as a rigid spherical body and was simulated by a "ball" element. The protective structure was simplified to a rigid slab and was represented by a "wall" element. The sand cushion was simulated by a large number of spherical particles. Therefore, the size of the spherical particles was a key parameter. The actual size of the sand grain was approximately 0.1 mm. However, it was unpractical to simulate the sand cushion with the particle size of 0.1 mm, especially in the actual engineering scale. Naito et al. [18] examined the effect of the particle size of the sand on the maximum impact force and defined K as the ratio of the diameter of the falling block to the maximum diameter of the sand particle. The results indicated that the larger particle size of the sand, the lower the impact force. Moreover, when the value of K was higher than 10, the value of the maximum impact force stabilized. Therefore, in the simulation of the sand cushion by the DEM model, we set the particle size of the sand to the higher value than the actual grain size of the sand.

The mechanical parameters that were used in DEM model were equally important. In continuum methods, a constitutive model is generally applied to describe the mechanical behavior of a material, and relevant parameters or curves are obtained through laboratory tests. However, the DEM model that was built in the PFC3D software was unable to directly embed macro constitutive models or mechanical parameters into the sand cushion model. Moreover, basic contact parameters (Fig. 1) are difficult to obtain from experimental results. Due to the complexity of the sand meso-structure and the limitation of the research, the researchers did not obtain a reliable mechanical theory to establish a quantitative relationship between meso parameters and macro parameters. Currently, the most common method to determine basic contact parameters is

the transformation of the macroscopic mechanical properties of samples or large-scale experiments via trial-and-error approach [23].

2.2 The Validation of the Model

To ensure the reliability of the simulation method developed in this paper, we validated the DEM model and model parameters by a real-scale prototype experiment [9]. In the experiment, a spherical falling block with a diameter of 0.9 m and a mass of 850 kg was dropped on a sand stratum that covered a rigid concrete plate embedded into the ground. The sand was compacted to the thickness of 2 m. To investigate the effect of the falling height on the dynamic response of the structure, five falling heights were arranged and the impact position was maintained. After each impact test, the crater induced by the impact of the rockfall was replenished and compacted. Then, the influence of the previous impact test on the following test was neglected. The detail of the real-scale experiment is described in the relevant thesis [9].

The above mentioned experiments employed the PFC3D software to simulate the impact of the rockfall. The three-dimensional numerical model is shown in Fig. 2. The radius of the particle ranged from 2–4 cm to ensure that the value of K was higher than 10. When the width of the sand cushion is four times the diameter of the falling block, the influence of lateral boundaries can be neglected [24]. In the DEM model, the width of the sand cushion was set to 5 m and the number of the element was set to 112,334. By repeatedly adjusting contact parameters (the effective modulus, the normal-to-shear stiffness ratio, and the friction coefficient) and the damp coefficient of the ball, we obtained a good agreement between simulation results and experimental results (Table 1 and Fig. 3). The simulation parameters that were used in the DEM model are listed in Table 2.

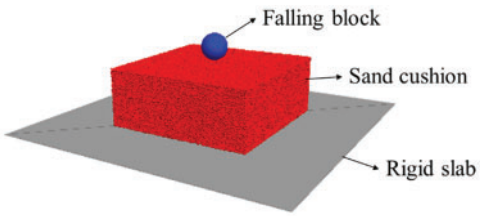

Figure 2: The numerical model of the impact of the rockfall

On the basis of the numerical simulations, we obtained the values of the maximum impact force under the five values of the falling height (Table 2). As shown in Table 2, simulation results are consistent with experimental results. The average error is 5% and the maximum error is below 10%. For example, the evolution of the impact force at the falling height of 36.4 m is shown in Fig. 3a. Herein, the impact force was defined as the force of the falling block that acted on the sand cushion. When the rigid block hits the sand cushion, the impact force quickly increases. Because the grain size of the model was higher than the actual grain size, the increase rate of the impact force that was obtained by experiments was higher than that obtained by the simulation. After the impact force reaches the maximum value, it gradually decreases to zero. At this stage, the two curves exhibit a similar characteristic. Fig. 3b shows the relationship between the penetration depth of the falling block and the falling height. In the real-scale experiment, the penetration depth was measured by the depth of the crater induced by the impact. Under the low impact energy (i.e., the low falling height), there is a small difference between the penetration depth

obtained from the simulation and the experiments. When the falling height increases, the difference increases, and the maximum error was approximately 20% (by a few centimeters). The comparison of the penetration depth required a more accurate experimental measurement.

Table 1: The experimental value and the numerical simulation value of the maximum impact force

Falling height/m	Maximum impact force/MN		Error $(F_1–F_2)/F_1$
	Experimental value (F_1)	Numerical simulation value (F_2)	
4.9	0.49	0.46	6%
6.3	0.55	0.54	2%
8.6	0.64	0.67	−5%
19.4	1.05	1.15	−9%
36.4	1.73	1.76	−2%

According to the above analysis, we obtained an acceptable agreement between simulation results and experimental results. Therefore, we concluded that the three-dimensional DEM model developed in this paper was reliable to simulate the impact process of the rockfall.

Table 2: Simulation parameters

Parameter	Value
Sand particle radius, m	0.02–0.04
Rock particle radius, m	0.45
Sand particle density, kg/m^3	2,228
Rock particle density, kg/m^3	2,500
Sand porosity, %	5
Effective modulus, N/m^2	2E7
Normal-to-shear stiffness ratio	1
Friction coefficient	0.1
Damp coefficient	0.7

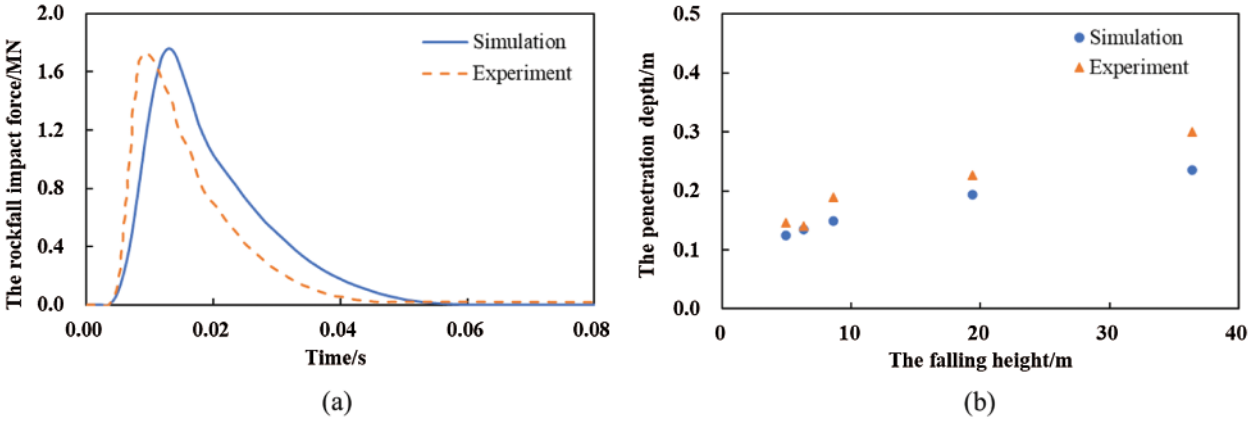

Figure 3: The numerical simulation results and the experiment results of: (a) the impact force of the rockfall at the falling height of 36.4 m; and (b) the penetration depth under the different falling height

3 Numerical Simulation Results

Analyzing numerical simulation results, we discussed the buffer performance of the sand cushion, the impact force of the rockfall, and the force that acted on the slab. The force that acted on the slab was a critical parameter for the design of the protective structure. Additionally, we discussed the effect of the properties of the sand cushion (the sand porosity and the cushion thickness) on the buffer performance of the sand cushion.

3.1 Simulation Cases

On the basis of the validation of simulation results by experimental results, we maintained the parameters related to the falling block and the sand cushion (except the thickness of the sand cushion) in the DEM model. To study the effect of the cushion thickness on the rockfall impact, we set the cushion thickness to 0.2, 0.4, 0.6, 0.8, 1.0, 1.5, 2.0 and 2.5 m, respectively. Moreover, we considered the different densities of the sand, which is described by the porosity of 0.05 (the dense sand), 0.2 (the medium sand) and 0.35 (the loose sand). The maximum and the minimum number of elements were 140,445 and 7,700, respectively. Twenty-four types of the sand cushion were simulated in this paper. The buffer performance of the sand cushion was tested under the five values of the falling height (10, 20, 30, 40 and 50 m). The analysis involved a total of 80 combinations of the operating conditions.

3.2 The Dynamic Process of the Impact of the Rockfall

Fig. 4a shows the variation in the impact force of the rockfall at the falling height of 50 m. As shown in Fig. 4a, once the falling block hits the sand cushion, the impact force increases quickly. After the impact force increases to the maximum value (Fig. 5a), the impact force gradually decreases until the two objects are separated from each other (Fig. 5b). The interval between the two stages was referred to as the impact time. The effect of the sand porosity (n) on the impact time is negligible. However, the thicker the sand cushion, the longer the impact time. In the first stage, the low sand porosity ($n = 0.05$) induces the increase rate of the impact force, of which the increase rate is independent of the cushion thickness. In the second stage, the impact force of the thin sand cushion is initially higher and then lower than the impact force of the thick sand cushion. The trend in variation of the impact force is exhibited by the dense and the loose sand cushion. During the impact, the force that acted on the rigid slab was defined as the cushion force, and the curves shown in Fig. 4b display the evolution of the cushion force. When the cushion thickness is similar, the sand porosity has little effect on the variation in the cushion force. Compared with the thin sand cushion, the thick sand cushion exhibits less variation in the cushion force. The maximum values of the impact force and the cushion force were the key issues that are discussed in the following sections.

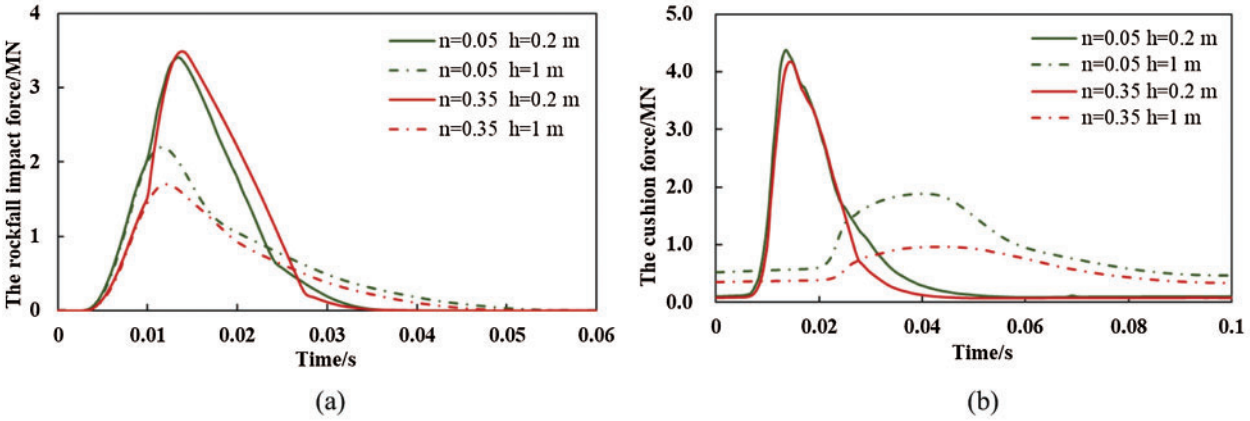

Figure 4: The evolution of (a) the impact force and (b) the cushion force

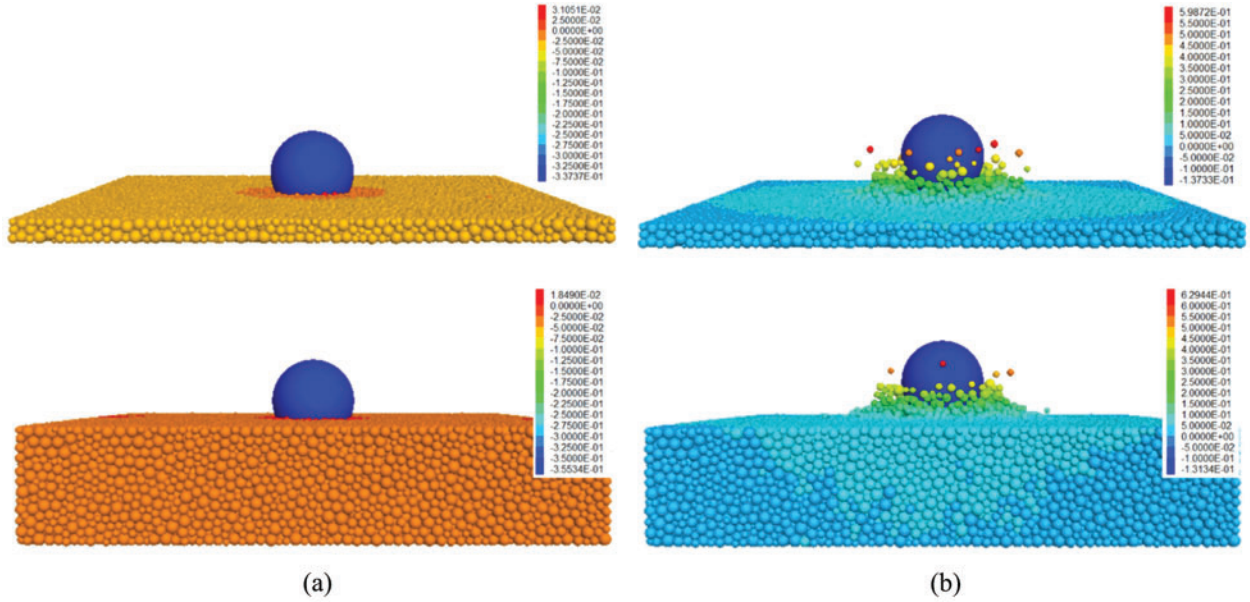

Figure 5: The dynamic impact process of (a) the decrease in the velocity of the falling block to zero and (b) the rebound of the falling block from the sand cushion. The color bars indicate the displacement of the balls

3.3 The Maximum Impact Force of the Rockfall

Fig. 6 shows the values of the maximum impact force (F_{max}) under the different thickness of the sand cushion. The values of the F_{max} of the sand cushion with the lowest thickness ($h = 0.2$ m) are very high. The increase in the cushion thickness to $h = 0.4$ m quickly decreases the F_{max} due to increase the buffer performance of the sand cushion. However, the increase in the cushion thickness to $h = 0.6$ m has little effect on the F_{max} of the sand cushion, especially at the range of the falling height value between 10 and 40 m. For the thick sand cushion ($h > 0.6$ m), the F_{max} remains constant due to the negligible buffer performance of the sand cushion. Moreover,

the dense sand cushion (Fig. 6a) and the loose sand cushion (Fig. 6b) express a similar trend in the variation of the F_{max}. In the practical engineering, the cushion thickness is higher than 0.6 m. Thus, we considered that the F_{max} was independent of the cushion thickness.

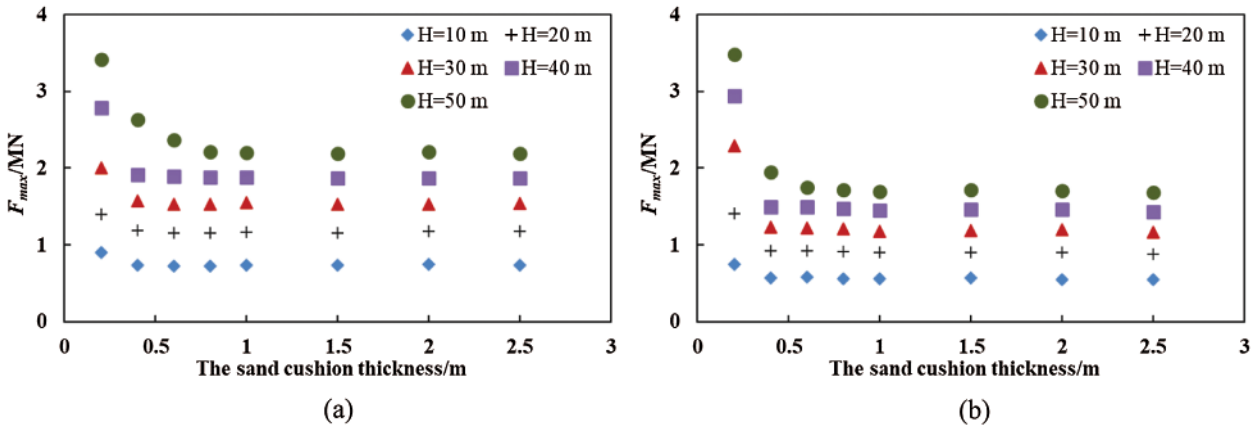

Figure 6: The F_{max} of (a) the dense sand cushion ($n = 0.05$) and (b) the loose sand cushion ($n = 0.35$) under the different cushion thickness

To explore the impact of the rockfall further, we regarded the average value of the F_{max} of the thick sand cushion ($h \geq 0.6$ m), the F_{ave}, as the nominal impact force. Fig. 7a shows the relationship between the F_{ave} and the falling height (H): the F_{ave} is a nearly linear function of the H. To investigate the effect of the sand porosity on the F_{ave}, we considered two types of the sand cushion, namely the dense sand cushion ($n = 0.05$) and the loose sand cushion ($n = 0.35$). The porosity is an important factor that affects the macroscopic mechanical properties of the sand. To resist the rockfall impact, the dense sand cushion generated higher deformation stiffness than did the loose sand cushion. As shown in Fig. 7a, the dense sand cushion ($n = 0.05$) generates higher F_{ave} than dose the loose sand cushion ($n = 0.35$). The dense sand cushion exhibited a relatively poor buffer performance. Under the high impact energy, the difference in the buffer performance of the two sand cushions increases. For example, when H is 10 m (Fig. 7a), the F_{ave} of the dense sand cushion is 0.73 MN and that of the loose sand cushion is 0.56 MN. When H increases to 50 m, the F_{ave} of the two sand cushions are 2.23 and 1.71 MN, respectively. Under the similar impact energy, the ratio of the F_{ave} of the dense sand cushion to that of the loose sand cushion is comparable. The F_{ave} of the dense sand cushion was approximately 1.3 times the F_{ave} of the loose sand cushion. Therefore, the loose sand cushion was more favorable to reduce the impact of the rockfall than the dense sand cushion.

The parameter ζ was defined as ($F_{0.2}$–F_{ave}), of which the $F_{0.2}$ was the maximum impact force at $h = 0.2$ m. The parameter ζ was used to describe the attenuation of the F_{ave} of a given sand cushion. The variation in the ζ with respect to the variation in the falling height is shown in Fig. 7b. A similar trend is observed for the sand cushion with the different sand porosity. When H is 10 m, the values of the ζ of the three sand cushions are similar. However, when H increases, the ζ of the dense sand cushion is lower than that of the loose sand cushion. The results indicate that when the thickness of the sand cushion increased from a low value ($h = 0.2$ m) to the designed value ($h > 1$ m), the F_{ave} of the sand cushion with the higher sand porosity decayed more quickly than did the F_{ave} of the sand cushion with the lower sand porosity.

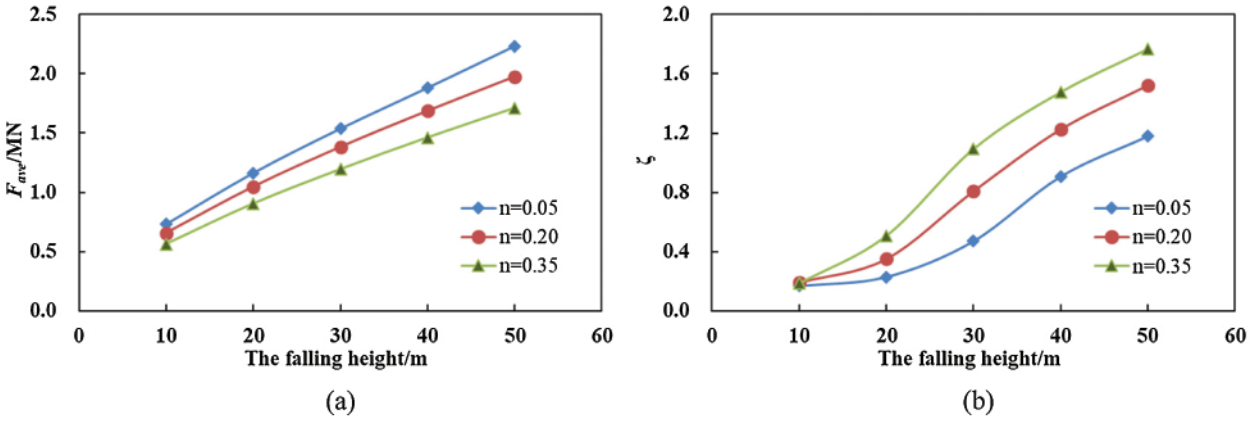

Figure 7: The effect of the sand porosity on (a) the F_{ave} and (b) the attenuation of the F_{ave}

3.4 The Bottom Force

When the rockfall hit the sand cushion, the impact force propagated quickly through the sand cushion and then acted as the external load on the structure. During the impact, the maximum force that acted on the rigid slab was defined as the bottom force (F_{bot}). The variation in the F_{bot} reflected the role of the sand cushion. The values of the F_{bot} under the different conditions are shown in Fig. 8. Unlike the variation in the F_{max} with respect to the cushion thickness, the variation in the F_{bot} exhibits a concave shape (except $H = 10$ m for the dense sand cushion). The F_{bot} consisted of two components, namely the dead load of the sand cushion and the force induced by the impact. When the cushion thickness is 0.2 m, the values of the F_{bot} are very high due to the poor buffer performance of the sand cushion, especially under the high impact energy. When the thickness of the sand cushion increases ($h = 0.4$–1.0 m), the F_{bot} decreases gradually due to the quick decrease in the impact force and the improvement on the buffer performance of the sand cushion. When the cushion thickness increases to $h = 1.0$–2.5 m, the F_{bot} remains approximately constant. Although the high thickness enhanced the buffer performance of the sand cushion, the additional force induced by the dead load of the sand cushion, which exceeded the buffer effect of the sand cushion, was significant. Therefore, as shown in Fig. 8, the F_{bot} gradually increases with the increase in thickness of the sand cushion. The effect of the cushion thickness and the falling height on the F_{bot} of the dense sand cushion and the loose sand cushion is similar. When H is 10 m, the curve that is shown in Fig. 8a is different from that shown in Fig. 8b. The F_{bot} of the dense sand cushion increases when the thickness of the sand cushion increases. In contrast, the F_{bot} of the loose sand cushion exhibits a concave shape when the thickness of the sand cushion increases. In the actual engineering practice, the evaluation of the appropriate cushion thickness should consider the effect of the buffer performance and the dead load of the sand cushion. Under the simulation condition (the falling height and the sand porosity) presented in this paper, we regarded that the appropriate thickness of the sand cushion was 1.5 m.

3.5 The F_{bot}/F_{max}

The sand cushion dissipates the impact energy of the rockfall and reduces the load that acts on the structure. Although the impact force can be calculated by several methods, the design of the rock shed is dependent on the F_{bot}. Currently, there are limited formulas to evaluate the F_{bot}. Thus, it is very important for designers to understand the relative magnitude of the F_{bot} and the F_{max}. Due to the dead load of the sand cushion and the complexity of the transmission of

the impact force through the sand cushion, the variation in the values of the F_{bot}/F_{max} (Fig. 9) is complex. When the thickness of the sand cushion increases, the F_{bot}/F_{max} curves, except the F_{bot}/F_{max} curve of the dense sand cushion at $H = 10$ m, exhibit three stages, namely the first rise stage, the decline stage, and the second rise stage. The minimum F_{bot}/F_{max} value occurs at the thickness of the sand cushion of 1.5 m. In the second stage, the increase in the impact energy quickly decreases the F_{bot}/F_{max}. However, in the third stage, the sand porosity influences the increase rate of the F_{bot}/F_{max}. The F_{bot}/F_{max} of the dense sand cushion is relatively stable, and under the high impact energy, the values of the F_{bot}/F_{max} can be regarded as a constant value (Fig. 9a). On the other hand, the F_{bot}/F_{max} of the loose sand cushion increases when the thickness of the sand cushion increases above 1.5 m (Fig. 9b).

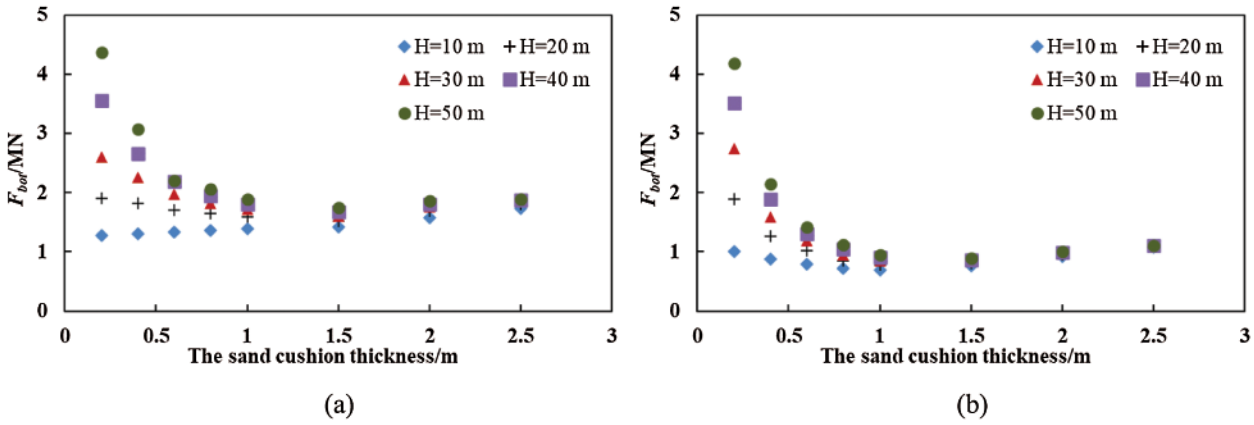

Figure 8: The F_{bot} of (a) the dense sand cushion ($n = 0.05$) and (b) the loose sand cushion ($n = 0.35$) under the different thickness of the sand cushion

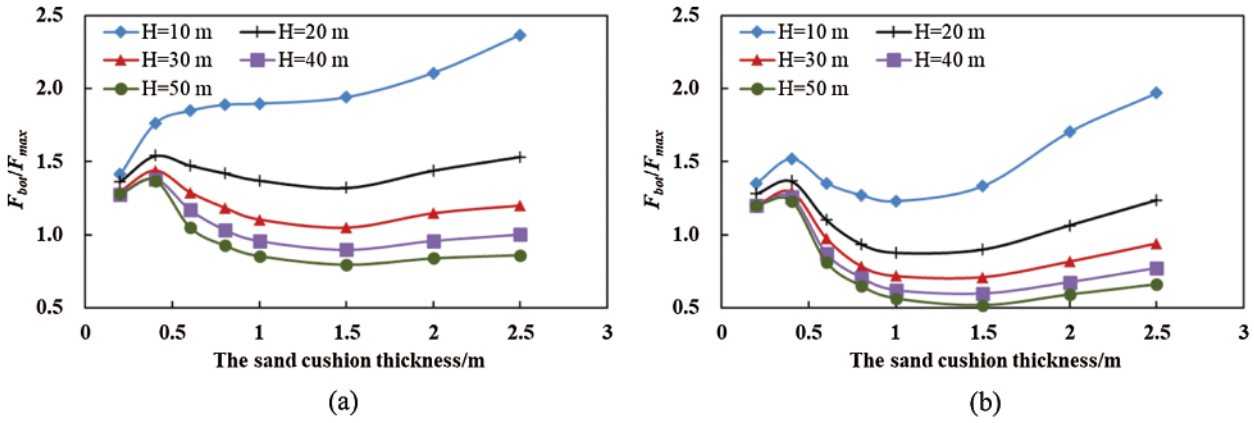

Figure 9: The F_{bot}/F_{max} of (a) the dense sand cushion ($n = 0.05$) and (b) the loose sand cushion ($n = 0.35$) under the different thickness of the sand cushion

The relative magnitude of the F_{bot}/F_{max} is shown in Fig. 10. As shown in Fig. 10, the effect of the falling height, the thickness of the sand cushion, and the sand porosity on the F_{bot}/F_{max} is highly significant. When the thickness of the dense sand cushion is $h \leq 0.6$ m, the F_{bot} is higher

than the F_{max} (Fig. 10a). When the thickness of the dense sand cushion increases to $h \geq 0.8$ m, under the low impact energy ($H \leq 30$ m), the F_{bot}/F_{max} is higher than 1, otherwise, the F_{bot} is lower than the F_{max}. Thus, when the value of the falling height is high and the sand cushion is thick, the F_{bot} is lower than the F_{max}. On the basis of the safety perspective, designers may regard the F_{max} as the force that acts on the structure. Except the F_{bot}/F_{max} of the loose sand cushion at $h < 0.6$ m and $H \leq 20$ m, the F_{bot}/F_{max} of the loose sand cushion is lower than 1 (Fig. 10b), which indicates that the approximation of $F_{bot} \approx F_{max}$ was applicable to the wider work condition.

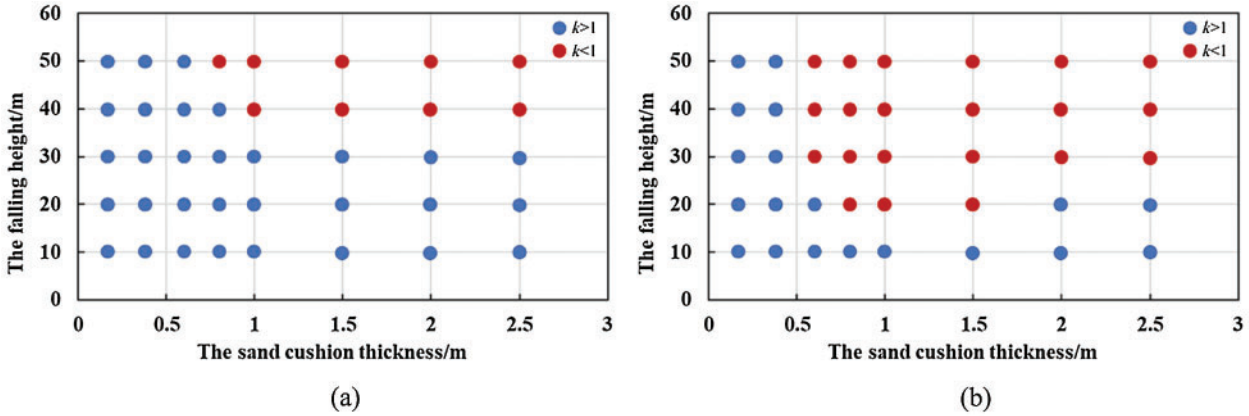

Figure 10: The ratio of the F_{bot} and the F_{max} ($k = F_{bot}/F_{max}$) of (a) the dense sand cushion ($n = 0.05$) and (b) the loose sand cushion ($n = 0.35$) under the different conditions

4 Discussion

When designing the rock shed, designers consider the F_{bot} an important load. Currently, the unclear magnitude of the F_{bot} is a major issue of the rock shed design. For designers, there are limited reliable reference methods to estimate the F_{bot}. Hence, the research on the F_{bot} is urgently needed. Generally, the F_{bot} consists of the static cushion dead load (F_{dead}) and the dynamic F_{add} induced by the impact of the rockfall. Unlike the simple calculation of the F_{dead}, the calculation of the F_{add} involves the complex dynamic process and the sand deformation property; thus, the F_{add} is difficult to estimate. In the practical engineering, a simple and practical method to evaluate the F_{add} is urgently needed.

Fig. 11 shows the values of the F_{add} ($F_{add} = F_{bot} - F_{dead}$) under the different conditions. When the thickness of the sand cushion increases, the F_{add} stabilizes, which indicates that the F_{add} hardly contributed to the increase in the F_{bot} when the thickness of the sand cushion increased. For example, as shown in Fig. 12, when the thickness of the sand cushion increases from 0.2 m to 2.5 m, the F_{add}/F_{bot} of the dense sand cushion decreases from 92% to 25% and the F_{add}/F_{bot} of the loose sand cushion decreases from 93% to 18%. Moreover, the F_{add}/F_{bot} is insignificantly affected by the falling height. Therefore, we concluded that when the thickness of the sand cushion was very high, the contribution of the F_{add} to the increase in the F_{bot} could be ignored; thus, the load that acted on the structure was easily identified and the difficulty of the structural design was greatly reduced.

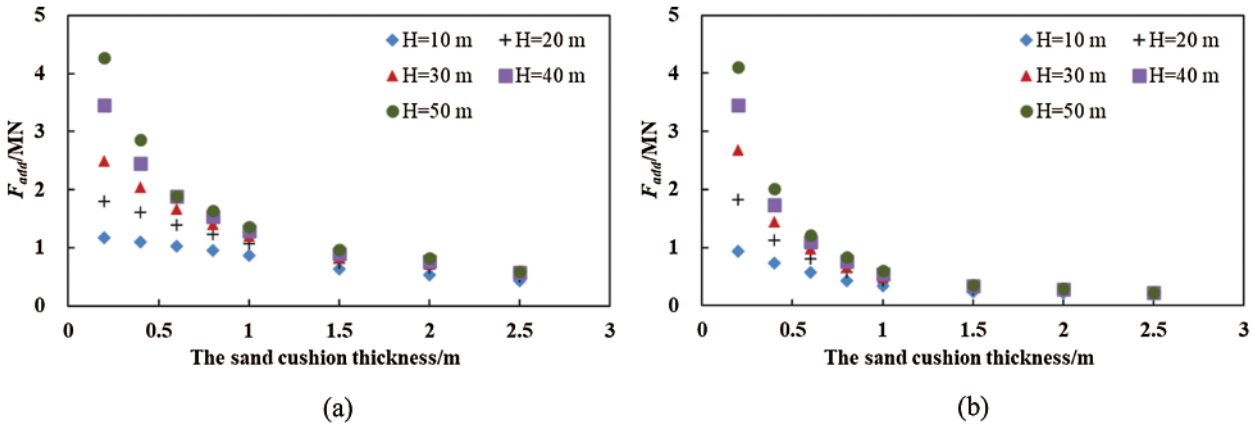

Figure 11: The F_{add} of (a) the dense sand cushion ($n = 0.05$) and (b) the loose sand cushion ($n = 0.35$) under the different cushion thickness

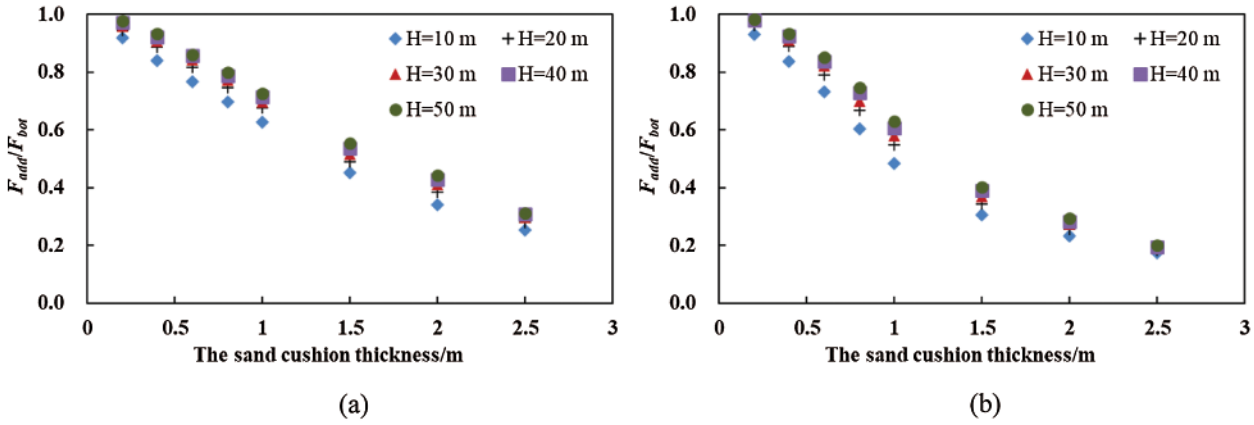

Figure 12: The F_{add}/F_{bot} of (a) the dense sand cushion ($n = 0.05$) and (b) the loose sand cushion ($n = 0.35$) under the different cushion thickness

To improve the structural safety and the structural resistance to the extreme impact load that is greater than the design load, designers should consider the F_{add}. Hence, we evaluated the relationship between the F_{add} and the F_{dead} to simplify the estimation of the F_{add}. On the basis of simulation results, we obtained the values of the F_{add}/F_{dead} under the different thickness of the sand cushion (Fig. 13). As shown in Fig. 13, the variation in the F_{add}/F_{dead} with respect to the variation in the cushion thickness is linear. At $h = 2.5$ m, the values of the F_{add}/F_{dead} under the range of the falling height value between 10 and 50 m are comparable, which indicates that the estimation of the F_{add} of the thick sand cushion was more convenient and simpler than was that of the F_{add} of the thin sand cushion.

However, the actual impact of the rockfall is more complex than is the impact of the rockfall simulated by the numerical model presented in this paper. In the future work, the numerical simulation will be conducted under the higher impact energy and the multi-impact process. Moreover,

the shape of the falling block and the properties of the sand cushion will be considered in the numerical model to replicate the actual engineering design.

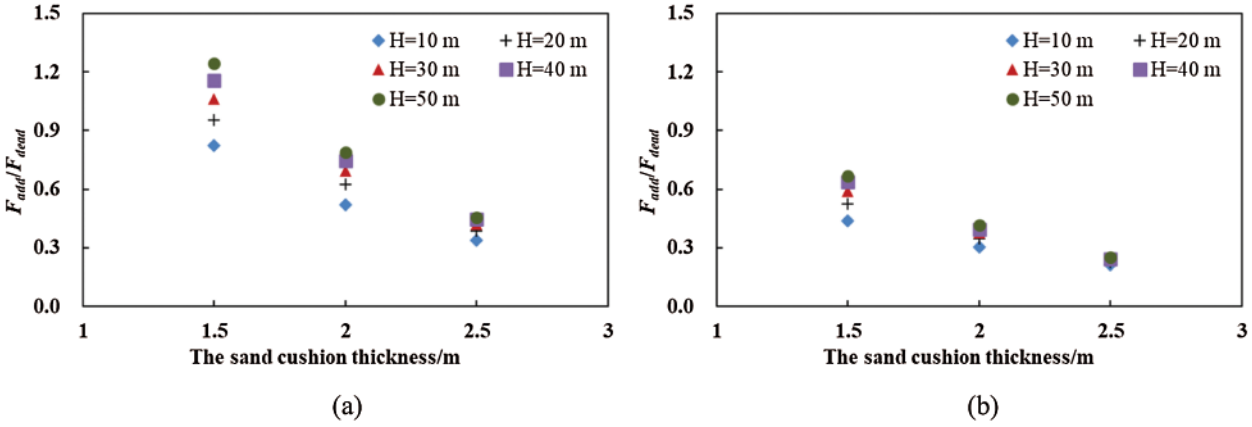

Figure 13: The F_{add}/F_{dead} of (a) the dense sand cushion ($n = 0.05$) and (b) the loose sand cushion ($n = 0.35$) under the different cushion thickness

5 Conclusions

The numerical analysis presented in this paper focused on the dynamic response of the sand cushion to the impact of the rockfall, of which the main conclusions of the numerical analysis were:

(1) When the thickness of the sand cushion was increased above 1 m, the additional thickness had little effect on the buffer performance of the sand cushion. The dense sand cushion generated higher impact force than did the loose sand cushion. Under the high impact energy, the difference in the buffer performance of the dense and the loose sand cushion was more significant than that under the low impact energy. When the thickness of the sand cushion increased from a low value to the designed value, the impact force of the dense sand cushion decayed more quickly than did the impact force of the loose sand cushion.

(2) The variation in the bottom force with respect to the variation in the cushion thickness was depicted by a concave curve. Although the high thickness enhanced the buffer performance of the sand cushion, the additional force contributed by the dead load of the sand cushion was significant. For the dense and the loose sand cushion, the effect of the cushion thickness and the falling height on the bottom force was similar. In the practical engineering design, we suggested designers to determine the appropriate thickness of the sand cushion on the basis of the buffer performance and the dead load of the sand cushion.

(3) When the thickness of the sand cushion increased, three stages were observed on F_{bot}/F_{max} curves, namely the first rise stage, the decline stage, and the second rise stage. Among the three stages, the second rise stage exhibited the most significant difference in the F_{bot}/F_{max} of the dense sand cushion and the loose sand cushion. The influence of the falling height, the thickness of the sand cushion, and the sand porosity on the F_{bot}/F_{max} was highly significant. The $F_{bot} \approx F_{max}$ simplification that is used in the actual engineering design should be examined carefully.

(4) When the cushion thickness increased, the F_{add} hardly contributed to the increase in the F_{bot}. The variation in the F_{add}/F_{dead} with respect to the variation in the thickness of the sand cushion was approximately linear. When the thickness of the sand cushion was above 2 m, the values of the F_{add}/F_{dead} under a range of the falling height value between 10 and 50 m were comparable, which indicated that the estimation of the F_{add} of the sand cushion with the high thickness was more convenient and simpler than that of the sand cushion with the low thickness.

Acknowledgement: We acknowledge the financial support from Sichuan Transportation Science and Technology Project (Grant Nos. 2020-MS3-101/2020-B-01 and 2019-ZL-12 and 2018-B-03) and the Science and Technology Department of Sichuan Province (Nos. 2021YFH0048 and 2021YFH0118).

Funding Statement: Sichuan Transportation Science and Technology Project (Grant Nos. 2020-MS3-101/2020-B-01 and 2019-ZL-12 and 2018-B-03) and the Science and Technology Department of Sichuan Province (Nos. 2021YFH0048 and 2021YFH0118).

Conflicts of Interest: The authors declare that they have no conflicts of interest to report regarding the present study.

References

1. Volkwein, A., Schellenberg, K., Labiouse, V., Agliardi, F., Berger, F. et al. (2011). Rockfall characterisation and structural protection: A review. *Natural Hazards and Earth System Sciences, 11(9),* 2617–2651. DOI 10.5194/nhess-11-2617-2011.
2. Zhao, P., Xie, L. Z., He, B., Zhang, Y. (2018). Experimental study of rock-sheds constructed with PE fibres and composite cushion against rockfall impacts. *Engineering Structures, 177(9),* 175–189. DOI 10.1016/j.engstruct.2018.09.073.
3. Yuan, S., Zheng, G. Q., Zhang, S., Li, L. P. (2019). Lessons learnt from disease and treatment engineering of opencut (Shed) tunnels in 10-years after Wenchuan Earthquake. *Tunnel Construction, 39(8),* 1372–1379. DOI 10.3973/j.issn.2096-4498.2019.08020.
4. Zhao, P., Yuan, S., Li, L. P., Ge, Q., Liu, J. et al. (2021). Experimental study on the multi-impact resistance of a composite cushion composed of sand and geofoam. *Geotextiles and Geomembranes, 49(1),* 45–56. DOI 10.1016/j.geotexmem.2020.09.004.
5. Kishi, N., Konno, H., Ikeda, K., Matsuoka, K. G. (2002). Prototype impact tests on ultimate impact resistance of PC rock-sheds. *International Journal of Impact Engineering, 27(9),* 969–985. DOI 10.1016/S0734-743X(02)00019-2.
6. Mougin, J. P., Perrotin, P., Mommessin, M., Tonnelo, J., Agbossou, A. (2005). Rock fall impact on reinforced concrete slab: An experimental approach. *International Journal of Impact Engineering, 31(2),* 169–183. DOI 10.1016/j.ijimpeng.2003.11.005.
7. Delhomme, F., Mommessin, M., Mougin, J. P., Perrotin, P. (2005). Behavior of a structurally dissipating rock-shed: Experimental analysis and study of punching effects. *International Journal of Solids and Structures, 42(14),* 4204–4219. DOI 10.1016/j.ijsolstr.2004.12.008.
8. Zineddina, M., Krauthammer, T. (2007). Dynamic response and behavior of reinforced concrete slabs under impact loading. *International Journal of Impact Engineering, 34(9),* 1517–1534. DOI 10.1016/j.ijimpeng.2006.10.012.
9. Calvetti, F., di Prisco, C. (2012). Rockfall impacts on sheltering tunnels: Real-scale experiments. *Geotechnique, 62(10),* 865–876. DOI 10.1680/geot.9.P.036.

10. Lambert, S., Gotteland, P., Nicot, F. (2009). Experimental study of the impact response of geocells as components of rockfall protection embankments. *Natural Hazards and Earth System Sciences, 9(2),* 459–467. DOI 10.5194/nhess-9-459-2009.
11. Kawahara, S., Muro, T. (2006). Effects of dry density and thickness of sandy soil on impact response due to rockfall. *Journal of Terramechanics, 43(3),* 329–340. DOI 10.1016/j.jterra.2005.05.009.
12. Zhao, P., Xie, L. Z., Li, L. P., Liu, Q., Yuan, S. (2018). Large-scale rockfall impact experiments on a RC rock-shed with a newly proposed cushion layer composed of sand and EPE. *Engineering Structures, 175(14),* 386–398. DOI 10.1016/j.engstruct.2018.08.046.
13. Calvetti, F., di Prisco, C., Vecchiotti, M. (2005). Experimental and numerical study of rock-fall impacts on granular soils. *Rivista Italiana di Geotecnica, 4(4),* 95–109.
14. Zhang, G. C., Tang, H. M., Xiang, X., Karakus, K., Wu, J. P. (2015). Theoretical study of rockfall impacts based on logistic curves. *International Journal of Rock Mechanics and Mining Sciences, 78(8),* 133–143. DOI 10.1016/j.ijrmms.2015.06.001.
15. Ouyang, C., Liu, Y., Wang, D., He, S. M. (2019). Dynamic analysis of rockfall impacts on geogrid reinforced soil and EPS absorption cushions. *KSCE Journal of Civil Engineering, 23(1),* 37–45. DOI 10.1007/s12205-018-0704-4.
16. Bhatti, Q. A. (2018). Computational modeling of energy dissipation characteristics of expanded polystyrene (EPS) cushion of reinforce concrete (RC) bridge girder under rockfall impact. *International Journal of Civil Engineering, 16(11),* 1–8. DOI 10.1007/s40999-018-0304-1.
17. Yan, P., Zhang, J. H., Fang, Q., Zhang, Y. D. (2018). Numerical simulation of the effects of falling rock's shape and impact pose on impact force and response of RC slabs. *Construction and Building Materials, 160(4),* 497–504. DOI 10.1016/j.conbuildmat.2017.11.087.
18. Naito, N., Maeda, K., Konno, H., Ushiwatari, Y., Suzuki, K. et al. (2020). Rockfall impacts on sand cushions with different soil mechanical characteristics using discrete element method. *Soils and Foundations, 60(2),* 384–397. DOI 10.1016/j.sandf.2020.02.008.
19. Zhang, L., Lambert, S., Nicot, F. (2017). Discrete dynamic modelling of the mechanical behaviour of a granular soil. *International Journal of Impact Engineering, 103(4),* 76–89. DOI 10.1016/j.ijimpeng.2017.01.009.
20. Shen, W., Zhao, T., Dai, F., Jiang, M., Zhou, G. D. (2018). DEM analyses of rock block shape effect on the response of rockfall impact against a soil buffering layer. *Engineering Geology, 249(4),* 60–70. DOI 10.1016/j.enggeo.2018.12.011.
21. Cundall, P. A., Strack, O. D. L. (1979). A discrete numerical model for granular assemblies. *Geotechnique, 29(1),* 47–65. DOI 10.1680/geot.1979.29.1.47.
22. Itasca Consulting Group Inc. (2016). PFC3D–Particle flow code in three dimensions. *Version 5.0 User's Manual*. Minneapolis: ICG.
23. Zhao, P., Xie, L. Z., Fan, Z. C., Deng, L., Liu, J. (2021). Mutual interference of layer plane and natural fracture in the failure behavior of shale and the mechanism investigation. *Petroleum Science, 18(2),* 618–640. DOI 10.1007/s12182-020-00510-5.
24. Maeda, K., Hashiba, H., Karita, K., Ushiwatari, Y., Kawase, R. (2011). Impact force propagation behaviors of rock fall into horizontal granular mat using 2D-DEM. *Journal of Applied Mechanics, 67(2),* 355–364. DOI 10.2208/jscejam.67.I_355.